Proc. of the International Conference on Electrical, Computer, Communications and Mechatronics Engineering (ICECCME 2024)
4-6 November 2024, Male, Maldives

2024 4th International Conference on Electrical, Computer, Communications and Mechatronics Engineering (ICECCME) | 979-8-3503-9118-3/24/$31.00 ©2024 IEEE | DOI: 10.1109/ICECCME62383.2024.10796829

A Case Study: Designing and Analysing a 3kW Squirrel Cage Induction Motor with FEM

Bekir Dursun
Edirne Vocational College of Technical Sciences
Trakya University,
Edirne,Türkiye
bekirdursun@trakya.edu.tr

Ali Özdil
Department of Electrical and Electronics Engineering
Kirsehir Ahi Evran University
Kirsehir,Türkiye
ali.ozdil@ahievran.edu.tr

Aganyyaz Ovezgeldiyev
Department of Electrical and Electronics Engineering
Kirsehir Ahi Evran University
Kirsehir,Türkiye
ovezgeldiyev.aganyyaz@ogr.ahievran.edu.tr

***Abstract*— Induction motors are crucial in industrial and commercial applications due to their reliability, efficiency, and low maintenance requirements. They account for a significant portion of global energy consumption, making their optimization essential for enhancing energy efficiency and reducing operational costs. A careful balance of mechanical, electrical, and thermal factors is necessary in the design of a three-phase squirrel cage induction motor to achieve maximum performance. This paper presents the design and performance evaluation of a 3-kW Squirrel Cage Induction Motor engineered to meet the high-efficiency standards set by the International Electrotechnical Commission (IEC) under the IE3 classification. The motor features advanced materials and optimized geometries, resulting in reduced losses and improved thermal management.**

Keywords*— *Design, Efficiency, FEM, Induction Motor, Squirrel Cage

I. INTRODUCTION

Galileo Ferraris is credited with creating the first three-phase AC Induction Motor, IM, in 1885, and Nikola Tesla, an engineer, is credited with implementing it in 1887. Dolivo Dobrowolski created the first Asynchronous Motors also known as Induction Motors that could be used in electric drives in 1890 [1]. IMs are a well-established technology that have been the most popular traction motor topologies in the railway transportation sectors for the past nearly 50 years due to their affordability and straightforward design. [2].

The primary benefit of an IM is that it operates solely on electromagnetic induction, requiring no additional excitation. Due to the low resistance of the short-circuit rotor windings, even a slight slip causes the rotor's current to increase and generate a sizable motor torque. [1]. One drawback is that the engine produces less starting torque when it first starts up than what is specified. [1].

Induction motors can be classified into two group based on their rotor structure i.e., slip ring rotor and squirrel cage rotor [3] demonstrated in Fig. 1.

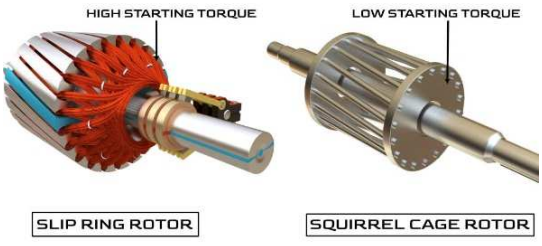

Fig. 1. Types of Induction Motors

Three-phase Squirrel Cage Induction Motors, SC-IMs, are extensively utilized in a variety of applications and are capable of powering various loads. The most common rotating electrical machine in the world, out of the hundreds of millions of electric motors, are these type of machines [4]. To implement the rotor-squirrel cage, three materials—aluminium, copper, and silumin—have been investigated in [5]. The findings indicate that adopting a copper cage increases efficiency by no more than 1.5% under rated load circumstances. [5].

Conventional vehicles contribute to several global issues, including global warming, noise pollution, pollution, and the depletion of fossil fuels. As a result, the automotive industry is now concentrating more on electric vehicles (EVs) [6]. Due to their many advantages over vehicles with internal combustion engines, electric vehicles are quickly becoming the standard. This particular field's bloom reduces pollution and contributes to a greener environment. The motor propulsion is the primary component of an electric vehicle that increases its competitiveness [7]. Importantly, electric vehicles (EVs) can be divided into four main categories: plug-in electric vehicles, fuel cell electric vehicles, battery electric vehicles, and hybrid electric vehicles (HEVs). For an electric vehicle to propel itself effectively, electric motors are essential. [8]. The different benefits and drawbacks of EVs were discussed in [7]. That study emphasises the promising future of technology in relation to electric vehicles [7]. Additionally, an electric vehicle-applicable optimized induction motor power loss model is presented in [7]. According to that study three variables: operating speed, electromagnetic torque, and stator reference flux are determined [9]. Out of all the losses in a pure electric car, the motor losses account for the majority. Therefore, in order to significantly lower the vehicle's energy consumption, it becomes necessary to eliminate those losses and extract the greatest amount of efficiency [9].

A traction electric motor, an energy storage unit (traction battery), and a power electronic converter (inverter) are the main parts of an electric vehicle's traction electric drive, TED [10]. Due to its exceptional efficiency and high-speed output performance, the Interior Permanent Magnet Synchronous Motor (IPMSM) can be regarded as a primary traction motor. Regarding the efficiency and performance of the high-speed output power, however, an IM with an identical stator is inferior. It does, however, show very low idling losses and little temperature variation in drag torque. Hence, an IM with a stator that is the same as an IPMSM can be used as an intermittent torque-generating auxiliary motor, especially at low speeds, like an engine-staring or four-wheel drive motor [11]. Because SC-IMs have the most advantageous qualities

such as simple construction, self-starting, affordability, high efficiency, and low maintenance, they are a fantastic substitute for electric vehicles [12]. On the other hand, Permanent Magnet Synchronous Machines, PMSMs, are utilized in electric vehicles due to their prominent features: high efficiency and torque capability, great power density thanks to the use of permanent magnets (PM). Nevertheless, because rare earths are scarce, the cost of these machines are extremely high [13].

The abovementioned beneficial characteristics of IMs points out that the design and analysis of these machine are climacteric. A system of non-linear equations pertaining to the motor's mechanical properties, performance, internal magnetic constraints, and thermal limitations make up the equation system that defines the motor design process [14]. These motors need to be designed and optimized, both mechanically and electrically, for them to function properly and operate at their highest efficiency [15]. IMs have four different and frequently used design class: Class A, B, C and D based on their rotor design and defined by National Electrical Manufacturers Association, NEMA. Among these classes, bars of a rotor belong to Class-A includes small bars placed near the rotor surface known as standard induction motor, with properties similar to a wound-rotor motor without the addition of additional resistance while those of Class-B are positioned deeply and they are larger comparing with the former ones demonstrated in Fig. 2 [3]. Besides, Class-C design can also be considered as double-cage rotor whereas small rotor bars are located close to the surface of rotor in Class-D shown in Fig. 2 [3].

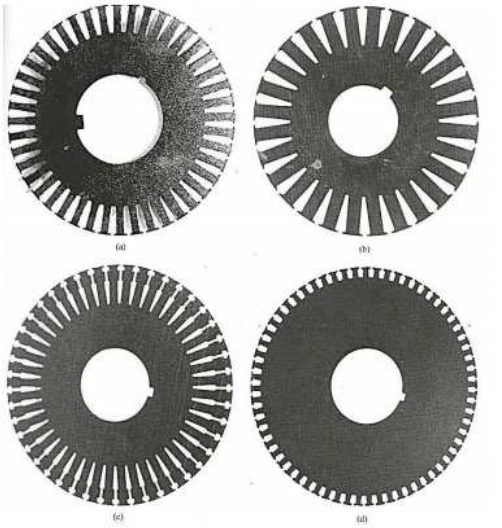

Fig. 2. NEMA design classes: A, B, C and D.

The IM design process and standard have reached a relatively mature state after years of development. Making substantial changes to the fundamental structure is challenging [16]. However, the analysis of IMs is still critical due to advantageous and highly using of these machines at industry. During the analysis of these machines. The unquestionable benefits of employing computers in the design of SC-IMs for specific applications—like electric vehicle propulsion—are highlighted in the specialty literature [17]. Finite Element Method, FEM, based software is frequently used to analyse electromagnetic systems and is sometimes necessary to investigate complex electromagnetic structures, like those found in rotating electric machines. The first FEM applications on electric machines date back to before the 1980s [8], when the computational capacity of the first powerful computers was a tiny portion of what is currently found in the least expensive notebooks on the market. FEM was very expensive and time-consuming to use at the time, and its applications were mostly restricted to the academic community, where universities were actively creating their own software for the sole purpose of conducting research [18]. However, it has been agreed by the recent researchers that FEM has spectacular features such as having the ability to visually represent flux paths and flux distribution. Moreover, this method supports to reduce cost of production of machines with realistic results, to save time with quick response and increase the efficiency of whole design process of an electrical machine [18].

The distribution of current density shown in Fig. 3, particular losses in the bars, and the heat release energy during the motor's start-up are crucial in the design of IMs and can all be found using numerical simulation [19]. The data from the analytical calculation are validated by the numerical simulation results for the current density distribution, specific losses, and stresses in the bar [19].

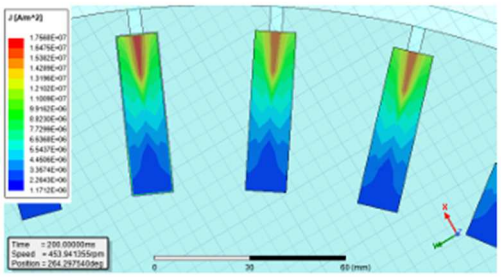

Fig. 3. An example of a current density of bars.

This study is a case study of analysis of a 3kW SC-IM consisting of four parts. The first part is an introduction to IMs; second part includes analytical investigation of these machines; third part is about the design procedure and applying FEM and the last part clarifies the conclusion and possible future works of the study.

II. Analytical Investigation of IMs

An induction motor operates by means of transformer action, which induces voltages and currents into the rotor circuit from the stator circuit [3]. The equivalent circuit of an induction motor will resemble the equivalent circuit of a transformer mostly because the induction of voltages and currents in the rotor circuit of an IM is fundamentally a transformer operation. A single-phase equivalent circuit of this type of machine is shown in Fig.4 [14].

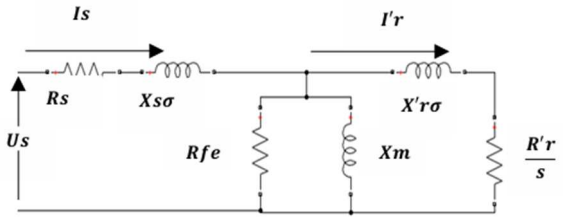

Fig. 4. Single Phase Equivalent Circuit of an IM.

The stator current and equivalent impedance of a single-phase IM can be calculated from the following equations [14]:

$$I_s = \frac{U_s}{Z_{eq}} \quad (1)$$

$$Z_{eq} = Z_s + \frac{Z_r^{`} * Z_m}{Z_r^{`} + Z_m} \quad (2)$$

where Z_s denotes stator impedance, Z_r' represent the value of the rotor impedance transferred to the stator and, the magnetization impedance is indicated by Z_m [14].

It is critical to investigate the power flow of IMs to evaluate the performance of these machines. The input, airgap, converted and out powers are respectively given by following equations [3]:

$$P_{in} = \sqrt{3} V_l I_l cos\theta \quad (3)$$

$$P_{ag} = P_{in} - P_{sc} - P_c \quad (4)$$

$$P_{cnv} = P_{ag} - P_{rc} \quad (5)$$

$$P_{out} = P_{cnv} - P_{fw} - P_{other} \quad (6)$$

where P_{in}, V_l, I_l, $cos\theta$, P_{ag}, P_{sc}, P_c, P_{cnv}, P_{rc}, P_{out}, P_{fw} and P_{other} denote input power, line voltage, line current, power factor, airgap power, stator copper loss, core loss, converted power, rotor copper, output power, friction-windage loss and stray loss, respectively.

The losses of an IM are classified into two categories i.e., electrical, and mechanical losses [3]. Electrical losses include stator copper, rotor copper and core losses. The square of the current passing through stator and rotor bars determines the predominant electrical losses in IMs. [19]. Since 3-phase SCIM is investigated, power losses are multiplied by three demonstrated in the following equations.

$$P_{ag} = 3I'^2_r \frac{R'_r}{s} \quad (7)$$

$$P_{rc} = 3I'^2_r R'_r \quad (8)$$

$$P_{sc} = 3I_s^2 R_s \quad (9)$$

$$P_{cnv} = 3I'^2_r R'_r (\frac{1-s}{s}) \quad (10)$$

The induced torque in IMs can be both obtained by following equations:

$$\tau_{in} = \frac{P_{cnv}}{\omega_m} \quad (11)$$

$$\tau_{in} = \frac{P_{ag}}{\omega_s} \quad (12)$$

where w_m and w_s denote rotor and synchronous speed of IMs. Moreover, the efficiency of these machines is given by:

$$\eta = \frac{P_{out}}{P_{in}} \quad (13)$$

III. FEM Analysis

In this part of the study, FEM analysis of a 3kW SC-IM was carried out. The specification of the motor is demonstrated in Table 1.

Table I. The motor specification.

Parameter	Value	Unit
Output Power	3	kW
Rated Voltage	400	V
Number of Poles	4	
Operating Frequency	50	Hz
Connection Type	Y	
Synchronous Speed	1500	rpm
Stator Slot Number	36	
Rotor Slot Number	32	
Design Class	A	
Slip	2.458	%
Operating Temperature	75	°C

The analysed motor was tested at rated values i.e., 50 Hz, 75°C and 400 V. The motor with 4 poles, 36 stator and rotor slots was designed to be in Class-A based on NEMA standards. Moreover, the slip of the Y-connected machine is 2.124 % with 1500 rpm synchronous speed.

Typically, thin, stacked, insulated laminations of premium steel make up the stator core. These laminations improve magnetic efficiency and decrease eddy current losses. The magnetic flux created by the stator windings finds a way through the core. The stator structure and winding connection of the analysed machine are shown in Fig. 5. To improve the performance of the designed machine double-layer structure is utilized in the stator slots shown in Fig. 5b.

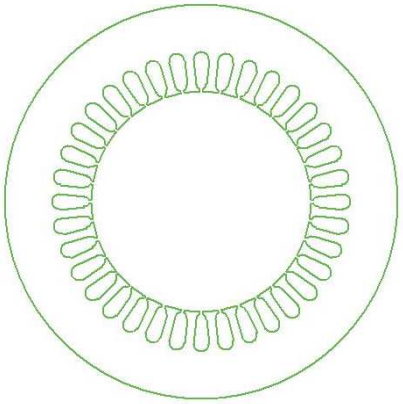

(a)

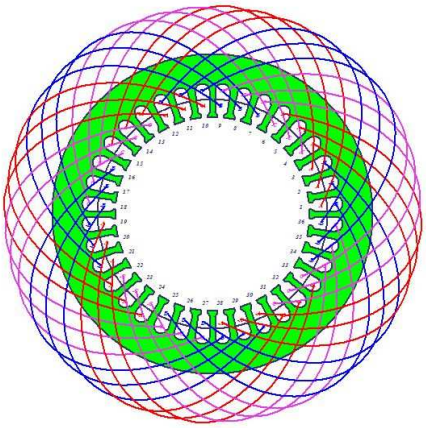

(b)

Fig. 5. a) Stator structure, b) Winding connection

A squirrel cage rotor's shape, composition, and arrangement of rods influence the motor's starting torque, efficiency, and operating characteristics. Because the rods are positioned at a specific angle to the rotor, the operation is more efficient, produces less noise, and improves starting performance. The rotor of the analysed SC-IM with 32 slots is demonstrated in Fig. 6.

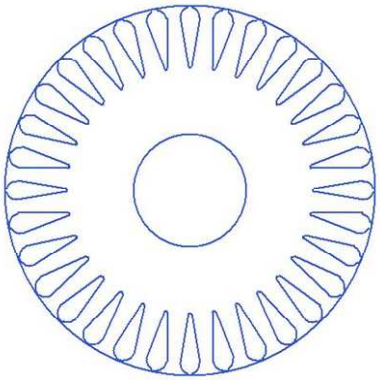

Fig. 6. Rotor Structure.

The analyses of machine were realized after the stator and rotor were created. The change of input current with the motor speed is illustrated in Fig. 7. The figure indicates that the current drawn by the machine decreases as speed augments. When the rotor speed reaches 1463 rpm, the machine is drawn 6.12A current.

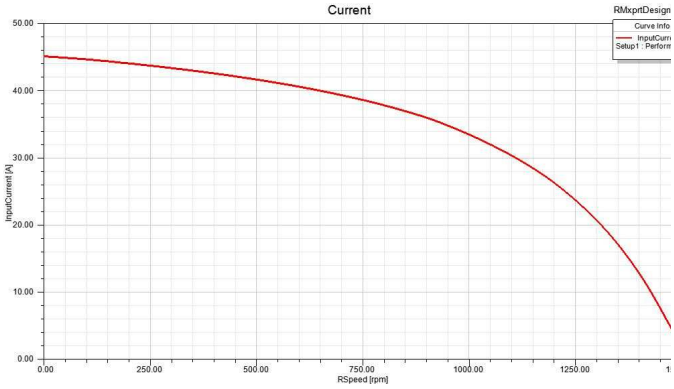

Fig. 7. Current-Speed relationship.

The change of torque with speed is demonstrated in Fig. 8. The maximum torque is obtained as 64.27 Nm at around 1125 rpm. This value is also known as breakdown torque of the machine and after that value the output torque is reduced. At the operating speed of the rotor, 1463 rpm, the produced torque is acquired as 19.38 Nm.

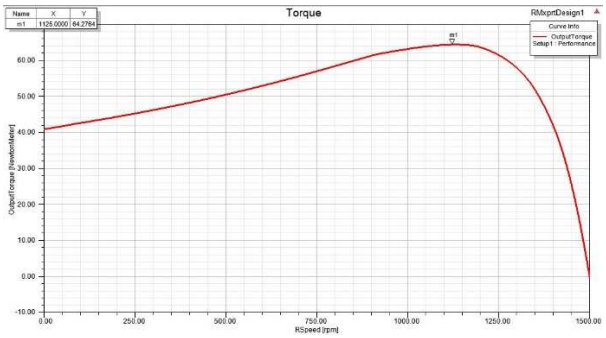

Fig. 8. Torque-Speed relationship.

Another important parameter needs to be investigated is the output power of the machine and the change of this power with speed is shown in Fig. 9. According to the figure, the maximum power is 8.037 kW obtained at 1245 rpm. At the rated speed of the rotor the output power is 3kW.

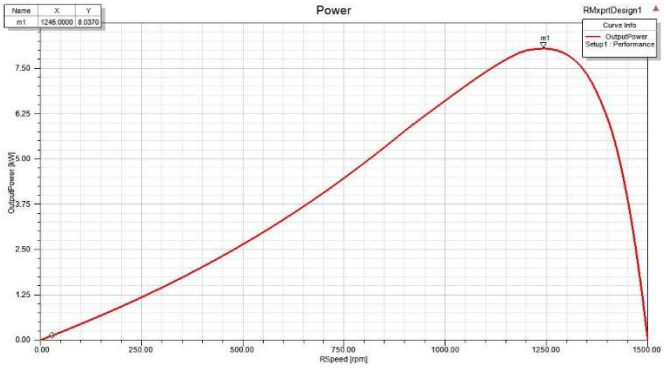

Fig. 9. Power-Speed relationship.

The analysis show that maximum torque and maximum power of the machine is obtained in different speeds. Having completed the analysis of current, torque and power of the machine with the change of rotor speed, 2-D analyses of the designed 3kW SC-IM were carried out. The duration of analyses is specified as 500 ms and the samples were taken at 0.005 s intervals. During the analyses the quarter part of the motor was used to save time illustrated in Fig.10.

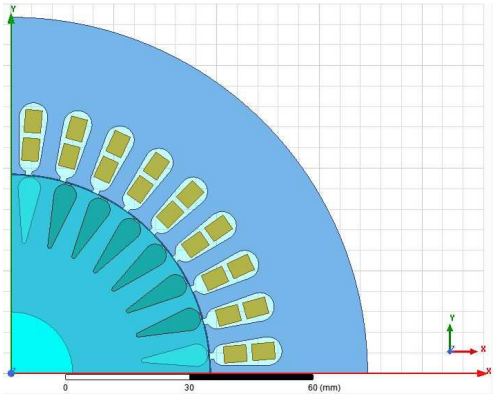

Fig. 10. The 2-D view of the motor.

The output torque of the motor is reached to its nominal value after 130 ms. The average value of the output torque and the torque ripple in the range of 200ms-500ms is respectively obtained as 19.6938 Nm and 13.51% shown in Fig. 11.

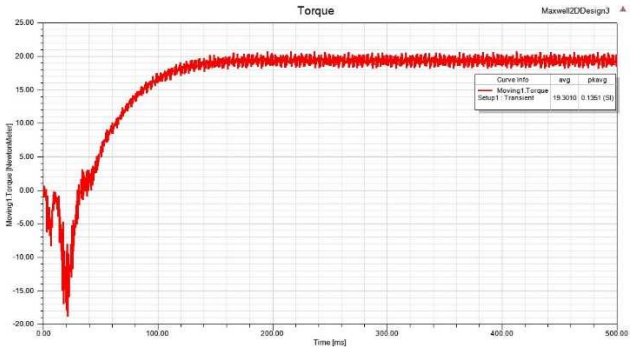

Fig. 11. Torque

Starting current for an asynchronous motor can range from five to eight times that of the motor's nominal load current. Asynchronous motors induce a significant amount of current in the rotor bars because, at the initial starting moment, the slip between the rotor and the magnetic field is at its maximum when the motor is in a stationary state. In addition, the motor draws a lot of current and runs with a very low impedance since no back-EMF is produced. The back-EMF rises and the current drawn gets closer to the nominal values as the motor speeds up [3]. The current drawn by the motor is quite high at starting conditions as explained above seen in Fig. 12. Similar to the torque graph, 3-phase currents are set closely to their nominal value as 6.24 A after 200 ms. Additionally, the shape of 120º shifted currents are almost purely sinusoidal.

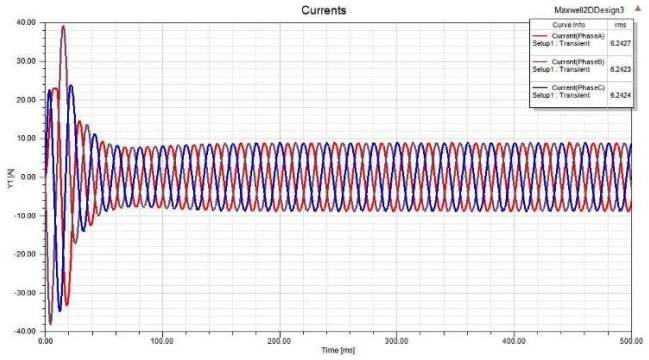

Fig. 12. Current.

The phase voltages induced in the designed machine and flux linkages of these phase are similarly 120^0 shifted and demonstrated in Fig. 13 and Fig. 14 respectively.

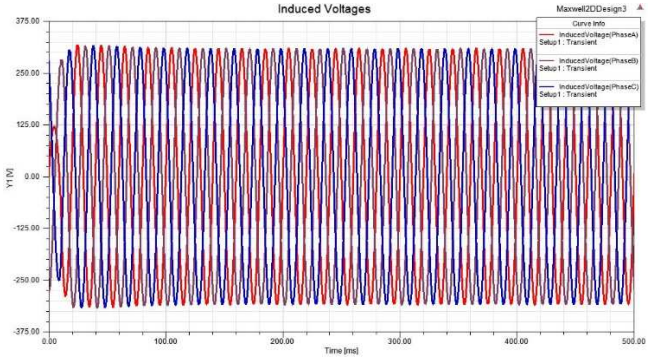

Fig. 13. Induced Voltage.

The obtained maximum value of flux linkages is around 0.98 Wb.

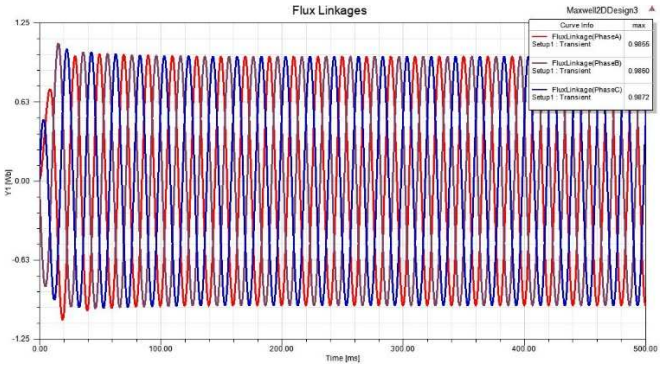

Fig. 14. Flux Linkage.

IV. Conclusions and Future Work

In this study, a 3kW SC-IM was designed and analysed via FEM. The motor with 36 stator and 32 rotor slots is placed in Class A. The results indicate that the maximum power and the maximum torque of the machine could be obtained in different speeds. The machine was drawn a high current at start-up and followingly was set to 6.24A. Moreover, torque and torque ripple were acquired as 19.6938 Nm and 13.51%, respectively. Additionally, the efficiency of designed motor is 89.323% within IE3 class and so close to IE4 class standardized by International Electrical Commission, IEC. Comparing with a study [20] of 3kW SC-IM having 36 stator and 30 rotor slots, the efficiency of designed motor in this study is 5.323% higher than that for obtained in [20]. Additionally, this study is approximately 7% more efficient than [21].

As a future work the efficiency of the machine can be improved by changing the class of the machine such as using Class B or C. The FEM analysed motor might also be implemented and analysed experimentally.

REFERENCES

[1] D. Iorgulescu, G. Samoilescu, V. Solcanu, M. Bălăceanu, C. Bărbulescu and A. Bordianu, "Applications of the Asynchronous Motor in the Anchoring Installation - Simulation and Advantages," 2020 International Symposium on Fundamentals of Electrical Engineering (ISFEE), Bucharest, Romania, 2020, pp. 1-6, doi: 10.1109/ISFEE51261.2020.9756133..

[2] F. S. Benavides, C. Madariaga, C. Gallardo and J. A. Tapia, "Electromagnetic Sizing Validation of Double Cage Induction Motor for Electric Vehicles Using Finite Element Simulation," 2023 IEEE CHILEAN Conference on Electrical, Electronics Engineering, Information and Communication Technologies (CHILECON), Valdivia, Chile, 2023, pp. 1-5, doi: 10.1109/CHILECON60335.2023.10418714.

[3] S. J. Chapman, Electric Machinery Fundamentals. 1985. [Online].Available: https://www.m5zn.com/newuploads/2014/09/13/pdf/6489ad501a3b6b0.pdf

[4] C. G. Dias, K. L. Rodrigues, N. C. Menegasse, W. A. L. Alves, and L. C. Da Silva, "Histogram of oriented gradients for rotor speed estimation in Three-Phase induction motors," IEEE Transactions on Instrumentation and Measurement, vol. 72, pp. 1–11, Jan. 2023, doi: 10.1109/tim.2023.3276530.

[5] G. Zeng et al., "Asynchronous machine with ferrofluid in gap: modeling, simulation, and analysis," IEEE Transactions on Magnetics, vol. 56, no. 1, pp. 1–4, Dec. 2019, doi: 10.1109/tmag.2019.2948614.

[6] A. Gupta, R. Machavaram, T. Kshatriya, and S. Ranjan, "Multi-Objective Design Optimization of a Three Phase Squirrel Cage Induction Motor for Electric Propulsion System using Genetic Algorithm," 2020 IEEE First International Conference on Smart Technologies for Power, Energy and Control (STPEC), Sep. 2020, doi: 10.1109/stpec49749.2020.9297776.

[7] H. Vidhya and S. Allirani, "A Literature Review on Electric Vehicles: Architecture, Electrical Machines for Power Train, Converter Topologies and Control Techniques," 2021 International Conference on Computational Performance Evaluation (ComPE), Shillong, India, 2021, pp. 565-575, doi: 10.1109/ComPE53109.2021.9751896

[8] M. D. S and V. Bagyaveereswaran, "Electric Motor Systems: Relative Study on Diverse Motors in the Electric Vehicles," 2023 Innovations in Power and Advanced Computing Technologies (i-PACT), Kuala Lumpur, Malaysia, 2023, pp. 1-6, doi: 10.1109/i-PACT58649.2023.10434509.

[9] S. Chourey, S. Bose and S. Sundaram, "An induction motor loss Optimization approach using JMAG and MATLAB for an electric vehicle," 2022 Interdisciplinary Research in Technology and Management (IRTM), Kolkata, India, 2022, pp. 1-5, doi: 10.1109/IRTM54583.2022.9791752.

[10] A. V. Klimov, V. V. Filatov, A. M. Tishin and D. A. Ptitsyn, "On Types of Traction Motors Used in the Leading Wheel Drive of Electric Passenger Vehicles," 2021 Systems of Signals Generating and Processing in the Field of on Board Communications, Moscow, Russia, 2021, pp. 1-5, doi: 10.1109/IEEECONF51389.2021.9416098.

[11] T. -K. Kim et al., "Experimental comparison of induction motor and IPMSM with identical stator," 2023 IEEE Energy Conversion Congress and Exposition (ECCE), Nashville, TN, USA, 2023, pp. 4208-4215, doi: 10.1109/ECCE53617.2023.10362907.

[12] T. S. S. S. Prakash and P. Krishna, "Asynchronous Cage Motor Performance Analysis using Ansys RMxprt," 2023 IEEE 3rd International Conference on Smart Technologies for Power, Energy and Control (STPEC), Bhubaneswar, India, 2023, pp. 1-6, doi: 10.1109/STPEC59253.2023.10430719.

[13] K. Li, A. Bouscayrol, S. Cui and Y. Cheng, "A Hybrid Modular Cascade Machines System for Electric Vehicles Using Induction Machine and Permanent Magnet Synchronous Machine," in IEEE Transactions on Vehicular Technology, vol. 70, no. 1, pp. 273-281, Jan. 2021, doi: 10.1109/TVT.2020.3047219.

[14] I. Laouar and A. Boukadoum, "Design Optimization of a Three-Phase Squirrel-Cage Induction Motor by Algorithm Harmony Search," 2022 IEEE International Conference on Electrical Sciences and Technologies in Maghreb (CISTEM), Tunis, Tunisia, 2022, pp. 1-6, doi: 10.1109/CISTEM55808.2022.10044025.

[15] H. Norry, A. Yildiz, S. Aksun and C. Aksoy, "Influence of Manufacturing Faults on Squirrel Cage Induction Motor," 2024 Fourth International Conference on Advances in Electrical, Computing, Communication and Sustainable Technologies (ICAECT), Bhilai, India, 2024, pp. 1-6, doi: 10.1109/ICAECT60202.2024.10469352.

[16] Y. Xu, Z. Xu and M. Ai, "Application of Ring Winding in Induction Motor," in IEEE Transactions on Applied Superconductivity, vol. 31, no. 8, pp. 1-5, Nov. 2021, Art no. 0603705, doi: 10.1109/TASC.2021.3107809.

[17] S. -M. Digă, V. Năvrăpescu, N. Digă and C. Dina, "Considerations on the Optimal Computer-Aided Design of Induction Motors from the Turbomachines Drive Systems in Power Plants," 2021 12th International Symposium on Advanced Topics in Electrical Engineering (ATEE), Bucharest, Romania, 2021, pp. 1-6, doi: 10.1109/ATEE52255.2021.9425259.

[18] E. B. Agamloh and A. Cavagnino, "High efficiency design of induction machines for industrial applications," 2013 IEEE Workshop on Electrical Machines Design, Control and Diagnosis (WEMDCD), Paris, France, 2013, pp. 33-46, doi: 10.1109/WEMDCD.2013.6525163.

[19] E. B. Agamloh and A. Cavagnino, "High efficiency design of induction machines for industrial applications," 2013 IEEE Workshop on Electrical Machines Design, Control and Diagnosis (WEMDCD), Paris, France, 2013, pp. 33-46, doi: 10.1109/WEMDCD.2013.6525163.

[20] T. M. Masuku, R. -J. Wang, M. C. Botha and S. Gerber, "Design Strategy of Traction Induction Motors," 2019 Southern African Universities Power Engineering Conference/Robotics and Mechatronics/Pattern Recognition Association of South Africa (SAUPEC/RobMech/PRASA), Bloemfontein, South Africa, 2019, pp. 316-321, doi: 10.1109/RoboMech.2019.8704761.

[21]H. M. Mzungu, A. B. Sebitosi and M. A. Khan, "Comparison of Standards for Determining Losses and Efficiency of Three-Phase Induction Motors," 2007 IEEE Power Engineering Society Conference and Exposition in Africa - PowerAfrica, Johannesburg, South Africa, 2007, pp. 1-6, doi: 10.1109/PESAFR.2007.4498051.